Author version: *Paleoceanography, vol.29(8); 2014; 778-794*

Late Holocene primary productivity and sea surface temperature variations in the northeastern Arabian Sea: implications for winter monsoon variability

Anna Böll[1*], Andreas Lückge[2], Philipp Munz[3], Sven Forke[4], Hartmut Schulz[3], V. Ramaswamy[5], Tim Rixen[1,4], Birgit Gaye[1], Kay-Christian Emeis[6,1]

1. Institute of Biogeochemistry and Marine Chemistry, University of Hamburg, Bundesstr. 55, 20146 Hamburg, Germany

2. Bundesanstalt für Geowissenschaften und Rohstoffe, Stilleweg 2, 30655 Hannover, Germany

3. Department of Geosciences, University of Tübingen, Hölderlinstr. 12, 72074 Tübingen, Germany

4. Leibniz Center for Tropical Marine Ecology, Fahrenheitstr. 6, 28359 Bremen, Germany

5. National Institute of Oceanography, Dona Paula, Goa 403004, India

6. Institute of Coastal Research, Helmholtz Center Geesthacht, Max-Planck-Str. 1, 21502 Geesthacht, Germany

Abstract

Variability in the oceanic environment of the Arabian Sea region is strongly 34 influenced by the seasonal monsoon cycle of alternating wind directions. Prominent and well studied is the summer monsoon, but much less is known about late Holocene changes in winter monsoon strength with winds from the northeast that drive convective mixing and highsurface ocean productivity in the northeastern Arabian Sea. To establish the first high resolution record of winter monsoon variability for the late Holocene, we analyzed alkenone derived sea surface temperature (SST) variations and proxies of primary productivity (organic carbon and $\delta_{15}N$) in a well-laminated sediment core from the Pakistan continental margin. Increased summer monsoon and weak winter monsoon intensities off Pakistan are indicated from 400 B.C. to 700 A.D. by reduced productivity and relatively high SST. At about 700 A.D. the intensity of the winter monsoon increased off Pakistan as indicated by a trend to lower SST. We infer that winter monsoon was still weak from 700 to 1400 A.D., because primary production did not increase despite decreasing SST. Declining SST and elevated biological production from 1400 to 1900 A.D. suggest invigorated convective winter mixing by strengthening winter monsoon circulation, most likely a regional expression of colder climate conditions during the Little Ice Age on the Northern Hemisphere. The comparison of winter monsoon intensity with records of summer monsoon intensity suggests that an inverse relationship between summer and winter monsoon strength exists in the Asian monsoon system during the late Holocene, effected by shifts in the Intertropical Convergence Zone.

Keywords

sea surface temperature, paleoproductivity, winter monsoon, late Holocene, northeastern Arabian Sea

1. Introduction

The Asian monsoon system is one of the most important components of global climate. Although variations in the Asian monsoon can have a great impact on climatological and biogeochemical processes in the ocean as well as on land, there are still only a few studies recording monsoon variability during the last 2000 years in high resolution. One opportunity to receive such high resolutions records of late Holocene climate change comes from laminated sediments deposited in the Makran area in the northeastern Arabian Sea [*von Rad et al.*, 1999; *Doose-Rolinski et al.*, 2001; *Lückge et al.*, 2001].

Primary productivity in the Arabian Sea, one of the most productive ocean basins worldwide, is strongly coupled to the seasonal dynamics of the Asian monsoon system, which is mainly forced by reversing atmospheric pressure gradients between continent and ocean accompanied by seasonal shifts in the Intertropical Convergence Zone (ITCZ) [*Clemens et al.*, 1991]. Strong south-westerly winds during the summer months caused by differential land-ocean heating in spring [*Hastenrath and Lamb*, 1979] lead to clockwise surface water circulation in the Arabian Sea and upwelling of nutrient rich waters along the coast off Somalia, Oman and southwest India. As a consequence, high biological productivity during the months June to September results [*Nair et al.*, 1989; *Haake et al.*, 1993]. A second primary productivity peak of minor importance occurs during the winter months as the wind directions reverses due to faster cooling of the content. Prevailing moderate and dry north-easterly winds lead to anti-clockwise surface circulation and to a cooling of Arabian Sea surface waters [*Wyrtki*, 1973] thereby initiating biological productivity associated to convective winter mixing [*Banse and McClain*, 1986; *Madhupratap et al.*, 1996].

Whereas most sediment trap studies in the central Arabian Sea indeed indicate highest biological productivity during the summer monsoon [*Broerse et al.*, 2000; *Prahl et al.*, 2000; *Wakeham et al.*, 2002], highest particle fluxes in the northeastern Arabian Sea are observed during the winter monsoon season [*Andruleit et al.*, 2000; *Lückge et al.*, 2002; *Schulz et al.*, 2002; *Rixen et al.*, 2005] and are associated with sea surface cooling down to about 23°C. Hence, periods of low sea surface temperatures (SSTs) in the northeastern Arabian Sea are linked to the cool northeast-monsoonal winds during winter.

We know today that monsoon activity varied not only on Milankovitch timescales but also during the late Holocene, as evident in Arabian Sea sediments [*von Rad et al.*, 1999; *Lückge et al.*, 2001; *Anderson et al.*, 2002, 2010; *Gupta et al.*, 2003; *Agnihotri et al.*, 2008; *Chauhan et al.*, 2010] and in various cave records from Oman [*Burns et al.*, 2002; *Fleitmann et al.*, 2004], Yemen [*Van*

Rampelbergh et al., 2013], India [*Sinha et al.*, 2007, 2011; *Berkelhammer et al.*, 2010] and China [*Zhang et al.*, 2008]. Similarly, primary productivity in the Arabian Sea was not uniform on timescales of a few hundred thousand years, but tracked monsoon variations caused by glacial/interglacial cycles [*Rostek et al.*, 1997; *Schulz et al.*, 1998; *Schulte et al.*, 1999; *Schulte and Müller*, 2001]. Although some knowledge exists about summer monsoon related changes in primary productivity over the last 2000 years from the Oman Margin [*Anderson et al.*, 2002, 2010; *Gupta et al.*, 2003] and the southwestern coast off India [*Agnihotri et al.*, 2008], paleoceanographic responses to late Holocene winter monsoon variability in the northeastern Arabian Sea are unknown.

Here we report the first high-resolution record of winter monsoon variability 103 for the late Holocene discerned from changes in primary productivity and sea surface temperature for the mainly winter monsoon dominated northeastern Arabian Sea. We analyzed a 188 cm long section of a well laminated sediment core from the Pakistan Margin for bulk components (organic carbon, carbonate and opal), stable nitrogen isotopes and alkenone unsaturation ratios to reconstruct productivity and monsoon variability throughout the last 2400 years. A key proxy for the winter monsoon intensity is the alkenone-derived SST estimate, which we validate by analyzing the seasonality of the alkenone SST signal at Eastern PAKOMIN sediment trap station (EPT-2) close to our core location. Our detailed objectives are to (1) examine the relationship between SST and alkenone unsaturation ratios in sediment trap material for the northeastern Arabian Sea; (2) reconstruct late Holocene (winter monsoon dominated) SST and paleoproductivity changes for the northeastern Arabian Sea; (3) compare the winter monsoon dominated record with records of summer monsoon variability to learn about the dynamics of the monsoon low-level wind system; and (4) examine possible links in the regional wind and surface ocean system to Northern Hemisphere climate change in historical time.

2. Study area

In the northeastern Arabian Sea (Pakistan Margin) SST persists warm during summer (27.8 to 29.3°C) but show a strong cooling of up to 23°C during the winter season. Cool winter SSTs are accompanied by a deepening of the mixed layer thereby indicating strong convective winter mixing during the northeast (NE) monsoon season (Fig. 2). Unlike the coast of Somalia, Oman and southeast India, no upwelling occurs during the southwest (SW) monsoon season on the Pakistan Margin. Thus, *Schulz et al.* [1996] concluded that primary production during summer is partly linked to the lateral advection of nutrient rich surface waters from the upwelling area off Oman. Seasonal productivity in the northeastern Arabian Sea peaks during the SW monsoon but also exhibits high values during the winter season due to an additional supply of nutrients through convection processes [*Banse and McClain*, 1986; *Madhupratap et al.*, 1996]. Increased particle fluxes during the months

January and February indicate even higher production during the NE monsoon season than during the SW monsoon season for the Pakistan Margin [*Andruleit et al.*, 2000; *Schulz et al.*, 2002, see Fig. 2]. Analysis of time-series observations showed that nitrate concentrations in the surface layers as well as concentrations of chlorophyll a and primary production in the euphotic zone coincide with mixed layer depth and wind suggesting a primarily physical control on carbon fixation in this part of the Arabian Sea [*Prasanna Kumar et al.*, 2001]. In winter a reduction in solar insolation and dry continental air brought by prevailing north-easterly winds result in enhanced evaporation leading to densification and cooling of surface waters. Resulting convection processes deepen the mixed layer which leads to upward transport of nutrients into the surface layers fueling the biological productivity [*Madhupratap et al.*, 1996; *Prasanna Kumar and Prasad*, 1996; *Prasanna Kumar et al.*, 2001].

Further characteristic for the northern Arabian Sea is the existence of a broad and stable mid-water oxygen minimum zone (OMZ) between 200 and 1200 meter water depth which is maintained by high biological production and subsequent decay of organic matter combined with the advection of oxygen-depleted water masses from the south as well as reduced vertical mixing caused by the input of warm, highly saline water masses from the Persian Gulf and the Red Sea [*Olson et al.*, 1993; *Schulz et al.*, 1996]. One prominent feature within the Arabian Sea OMZ is the occurrence of high rates of denitrification which can be estimated using sedimentary $\delta^{15}N$ values. Elevated denitrification caused by high biological production and reduced oxygen concentrations result in enriched sedimentary $\delta^{15}N$ values whereas reduced denitrification lead to depleted sedimentary $\delta^{15}N$ values [e.g., *Altabet et al.*, 1995; *Naqvi et al.*, 1998; *Suthhof et al.*, 2001; *Gaye-Haake et al.*, 2005].

Sediments deposited within the OMZ off Pakistan are characterized by well preserved, varve-like lamination with altering dark and light sediment layers as well as high input of lithogenic material originating from dust storms and/or river runoff [*von Rad et al.*, 1995, 1999; *Schulz et al.*, 1996]. After *Schulz et al*. [1996] dark laminea were deposited during the high productivity season of the late summer monsoon whereas light-colored laminea contain almost exclusively land derived materials which were deposited during the winter monsoon.

3. Methods

3.1. Sample collection and stratigraphy

In this study we investigated piston core 275KL and box core 39KG, both located within the center of the OMZ off the Pakistan coast. Box core 39KG (24°50.01'N, 65°55.01'E; 695 m water depth) was taken in 1993 during SONNE cruise 90 and was studied by *von Rad et al.* [1999], *Doose-*

Rolinski et al. [2001] and *Lückge et al.* [2001]. Piston core 275KL was retrieved from the same position in 1998 during SONNE cruise 130 (24°49.31'N, 65°54.60'E; 782 m water depth). We studied the first 188 cm of core 275KL and the first 15 cm of core 39KG thereby producing a continuous chronology of the last 2400 years. Core 275KL was continuously sampled in 0.5 cm intervals (sample resolution of 5 to 80 years) for bulk analysis (organic carbon, carbonate) and every third or fourth sample of this sample series was used for opal and stable nitrogen isotope measurements. Alkenones were measured on continuous 2 cm intervals in core 275KL. In core 39KG all parameters were analysed on 1 cm thick intervals (6 to 8 year resolution). All samples were freeze-dried and homogenized with mortar and pestle prior to analyses.

In addition to seasonal varves, core 275KL exhibits reddish-brown silt turbidites up to 5 cm thick and light gray short-event deposits (>1.5 mm thick) which consists of allochthonous lithotypes and were thought to originate from suspended sediments previously deposited on the shelf and upper slope [*Schulz et al.*, 1996; *von Rad et al.*, 1999]. When sampled, sediments containing these event deposits or turbidites were excluded from our dataset.

Varves, turbidites and event layers in our core are comparable to sediment layers observed in core 56KA from the same position. Core 56KA was already well dated by *von Rad et al.* [1999] based on varve counts combined with several conventional and AMS ^{14}C-datings. Our age model is based on eye-to-eye correlation of event deposit layers from both cores as stratigraphic tie points and interpolation between these tie points.

We further analyzed samples from the Eastern PAKOMIN sediment trap mooring station (EPT-2; 24°45.6'N, 65°48.7E; 590 m water depth) for alkenones and calculated alkenone fluxes as well as the $U^{K'}_{37}$-index to receive sea surface temperatures. EPT-2 trap was deployed from May 1995 to February 1996 and was studied by *Andruleit et al.* [2000] and *Schulz et al.* [2002].

3.2 Bulk components (organic carbon, carbonate, opal)

Total carbon was analyzed on a Carlo Erba 1500 elemental analyzer (Milan, Italy) with a precision of 0.2%. Total organic carbon (TOC) was measured with the same instrument after samples were treated with 1 mol L^{-1} hydrochloric acid (HCl) to remove inorganic carbon. Analytical precision for organic carbon was 0.02%. Carbonate carbon was calculated as the difference between total carbon and organic carbon. The content of carbonate carbon was then converted to calcite ($CaCO_3$).

Biogenic opal was determined by wet alkaline extraction of biogenic silica (BSi) using a variation of the DeMaster method [*DeMaster*, 1981]. About 30 g sediment per sample was digested

in 40 mL of 1% sodium carbonate solution (Na_2CO_3) in a shaking bath at 85°C. After 3 hours the supernatant was withdrawn and neutralized in 0.021 M HCl. The concentration of dissolved silica in subsamples was determined photometrically. Biogenic opal was calculated by multiplying the BSi concentrations with a factor of 2.4. The mean standard deviation based on duplicate measurements of samples is 0.17%. To ensure that BSi is not overestimated by mineral dissolution at low BSi concentrations, we analysed a few exemplary samples after 3, 4 and 5 hours and used a slope correction for the determination of BSi concentrations [*Conley*, 1998]. The amount of BSi was then estimated from the intercept of the line through the time course aliquots [*DeMaster*, 1981]. Results of slope corrected opal estimates showed that our opal concentrations were slightly overestimated by a mean of 0.13%. All bulk components are presented as weight %.

Mass accumulation rates of organic carbon were calculated by multiplying the dry bulk densities of the sediments (measured at the Department of Geosciences – University of Tübingen) with calculated sedimentation rates and the weight fraction of organic carbon

3.3. X-ray elemental analysis

XRF Core Scanner data were collected by XRF Core Scanner I at MARUM (University of Bremen) using a KEVEX Psi Peltier Cooled Silicon Detector and a KEVEX X ray tube with the target material molybdenum (Mo). Counts were acquired directly at the split core surface of the archive half every 2 mm down-core over an area of 0.2 cm2 with an instrument slit size of 2 mm using a generator setting of 20 kV, 0.087 mA and a sampling time of 30 seconds. The split core surface was covered with a polypropylene foil to avoid contamination of the XRF measurement unit and desiccation of the sediment.

3.4. Nitrogen stable isotope ratios

The ratio of the two stable isotopes of nitrogen ($^{15}N/^{14}N$) is expressed as $\delta^{15}N$, which is given as the per mil deviation from the N-isotope composition of atmospheric N_2 ($\delta^{15}N = 0‰$): $\delta^{15}N = [(R_{Sample}-R_{Standard})/R_{Standard}]*1000$, where R_{Sample} is the $^{15}N/^{14}N$ ratio of the respective sample and $R_{Standard}$ is the $^{15}N/^{14}N$ ratio of atmospheric N_2. $\delta^{15}N$ values were determined using a Finnigan MAT 252 gas isotope mass spectrometer after high-temperature flash combustion in a Carlo Erba NA-2500 elemental analyzer at 1100°C. Pure tank N_2 calibrated against the International Atomic Energy Agency reference standards IAEA-N-1 and IAEA-N-2, which were, in addition to an internal sediment standard, also used as working standards. Analytical precision based on replicate measurements of a reference standard was better than 0.1‰. Duplicate measurements of samples resulted in a mean standard deviation of 0.07‰.

3.5 Alkenones

Freeze dried and homogenized sediment samples (1 to 3g) were extracted two times for 5 min with methylenchloride (DCM) using an accelerated solvent extractor (ASE, Dionex; temperature 75°C, pressure 70 bar). Directly after extraction a known amount of internal standard (14-Heptacosanone) was added to the resulting extracts. The extracts were rotary-evaporated until near dryness and saponified with 5% methanolic potassium hydroxide (KOH) solution over night. The KOH solution was dried under a nitrogen flow, dissolved in DCM and cleaned over a silica gel column using DCM as eluent. The clean fraction containing the alkenones was dried under N_2 and taken up in n-hexane (50-150µL) prior to analysis. Alkenones were analysed by gas chromatography on an Agilent 6850 gas chromatograph (GC) equipped with a split-splitless inlet system and flame ionisation detector (310°C). Separation was achieved on a silica column (30 m x 0.1 µm film thickness x 0.32 mm ID; Optima1; Macherey-Nagel) using hydrogen as carrier gas (1 mL min^{-1}). The GC oven maintained at 50°C for the first minute and was then programmed from 50° to 230°C at 20°C min^{-1}, from 230° to 260°C at 4.5°C min^{-1} and from 260° to 320°C at 1.5°C min^{-1} followed by an isothermal period of 15 min. $C_{37:2}$ and $C_{37:3}$ alkenones were identified by comparing peak retention times between sediment samples and a working sediment standard. Quantification of alkenones was achieved by integrating the peak areas of the C_{37} alkenones and that of the internal standard (14-Heptacosanone). Since both the C_{37} alkenones and the internal standard are very similar in structure, no different response factors between the C_{27}-ketone and the C_{37} alkenones are assumed. Replicate extraction and measurement of a working sediment standard resulted in a mean standard deviation of 0.5°C. Alkenones were translated into sea surface temperature using the core top calibration for the Indian Ocean from *Sonzogni et al.* [1997a]: SST = $(U^{K'}_{37}-0.043)/0.033$ with $U^{K'}_{37} = C_{37:2}/(C_{32:2} + C_{37:3})$. Replicate extraction and measurement of a working sediment 256 standard resulted in a mean standard deviation of estimated SST of 0.5°C.

4. Results

4.1. Alkenone fluxes and $U^{K'}_{37}$ in sediment traps

Alkenone fluxes in EPT-2 between May 1995 and February 1996 ranged from 0.15 µg m^{-2} d^{-1} to 1.21 µg m^{-2} d^{-1} (see Fig. 3a). Peak fluxes occurred in May 1995 (1.21 µg m^{-2} d^{-1}) and during the late NE monsoon in January 1996 (0.92 µg m^{-2} d^{-1}) and February 1996 (0.94 µg m^{-2} d^{-1}). Alkenone fluxes for the months September and October could not be determined due to low amounts of sample material. Alkenone fluxes on the Pakistan continental margin track coccolith fluxes during the seasonal cycle [*Andruleit et al.*, 2000] with maxima at the onset of the summer and of the winter monsoon. This

underscores a strong link between primary and alkenone production. Alkenone (C_{37}) fluxes on the Pakistan Margin match those from the Oman Margin [*Wakeham et al.*, 2002], but are slightly lower than total alkenone (C_{37}, C_{38}, C_{39}) fluxes in the Central Arabian Sea [*Prahl et al.*, 2000]. Sediment trap studies from different parts of the Arabian Sea thus showed a strong coupling between coccolithophore (and alkenone) production and the seasonal cycle in this area [*Andruleit et al.*, 2000; *Broerse et al.*, 2000; *Prahl et al.*, 2000; *Wakeham et al.*, 2002].

This seasonality may bias the SST signal in sediments towards seasonal flux maxima, so that it may not be representative of the annual mean SST (AM-SST). In our set of trap samples covering the period from May 1995 to February 1996 the seasonal variability of alkenone-derived SST (26.1°C to 28.1°C; $U^{K'}_{37}$ from 0.904 to 0.971; Fig. 3b) is attenuated compared to observed SSTs which vary from 23.0°C to 29.2°C [*Reynolds et al.*, 2002]. In particular, monthly average alkenone SSTs deviate most from modern observed SSTs during the cold winter months of the trapping period in 1995/1996. The average alkenone SST of the sampling period is 27.4°C, which is slightly higher compared to the mean modern SST (27.0°C; see Figure 3b), which in turn is very close to the average mean SST from May to February obtained from the Levitus climatology [26.9°C; *Levitus and Boyer*, 1994]. Climatological annual mean SST (including the months missing in the trap investigation) is 26.4°C [*Levitus and Boyer*, 1994]. But because alkenones reflect an integrated 284 signal of the upper 0 to 50 m of the water column [*Sonzogni et al.*, 1997a], small deviations from actual sea surface temperature measurements are to be expected.

We have no conclusive explanation for the weak seasonality of alkenone SST in EPT- 2 samples, but state that sedimentary $U^{K'}_{37}$-measurements on the Pakistan Margin are best approximated by AM-SST. This conclusion is supported by $U^{K'}_{37}$-estimates for sediment trap samples from the central Arabian Sea [*Prahl et al.*, 2000] and by a compilation of sediment trap time series distributed over different oceanic regions worldwide [*Rosell-Melé and Prahl*, 2013]. Furthermore, measurements of sediment core tops, which were used to develop an alkenone calibration equation for the Indian Ocean, showed no significant differences between calculated production weighted temperature and AM-SST [*Sonzogni et al.*, 1997a, 1997b]. According to *Doose-Rolinski et al.* [2001] alkenone-derived SSTs measured in a Holocene section of a sediment core from the Pakistan Margin were best approximated by annual mean temperature as well.

4.2. Alkenone SST record in core 39KG/275KL

Alkenone SST vary between 26.9°C and 28.4°C ($U^{K'}_{37}$ 300 from 0.932 to 0.981) over the last 2400 years and thus lie well above the modern annual mean of 26.4°C [*Levitus and Boyer*, 1994]. *Conte et*

al. [2006] stated that a positive offset of reconstructed core top temperature (27.6°C for SO90-39KG) compared to atlas temperature is observed in several areas worldwide. It is alternatively explained by diagenetic alteration of alkenone ratios in the water column and/or surficial sediments, by lateral advection, or by variations in the seasonality and depth of alkenone production. In our view, diagenesis can be ruled out as a significant process affecting our $U^{K'}_{37}$ -estimates, because the offset was also observed between trap alkenone SST and modern AM-SST, and was furthermore confirmed by Mg/Ca temperatures [*Dahl and Oppo*, 2006]. Biasing of the alkenone signal by 309 alkenones produced and advected from the upwelling area off Oman may be a factor [*Andruleit et al.,* 2000], but coccolithore fluxes on the Pakistan Margin are only slightly enhanced during the SW monsoon season and the associated bias in the alkenone signal must be of minor importance as SSTs in the southeastern Arabian Sea remain relatively high during winter, lateral advection of water masses and alkenones from the southwest Indian coast (following the anticlockwise surface current established during the NE monsoon) on the other hand would result in a warm bias of alkenone SST on the Pakistan Margin during the winter.

Regardless of the absolute SST, Figure 4 illustrates relative SST variations around the overall mean of 27.7°C over the last two millennia. SSTs were high at around 28.2°C until 250 A.D., rapidly decreased and outlined a time period of low SST that lasted from 400 to 1000 A.D. After a rebound to >28°C between 1000 and 1300 A.D. the decline in SST continued until minimum temperatures (26.9°C) are registered during the 18th century. The minimum of our SST reconstruction at this time agrees with results obtained from a global climate proxy network, which suggests 0.3°C cooler SSTs than present during the Little Ice Age in the northeastern Arabian Sea [*Mann et al.*, 2009]. Our SST estimates after this minimum suggest a northern Arabian Sea warming tendency that persists to the present.

4.3. Records of Productivity

Our analytical approach to trace past productivity changes were based on TOC concentrations, $\delta^{15}N$ values, and the ratio of carbonate to opal. The range of TOC concentrations (1.0 and 2.0%) and $\delta^{15}N$ values (7.1 to 8.5‰) in the sediment cores at site 39KG/275KL (Figure 4) is characteristic of high productivity areas with a well developed OMZ and water column denitrification [e.g., *Naqvi et al.*, 1998; *Altabet et al.*, 1999; *Gaye-Haake et al.*, 2005] such as the northern Arabian Sea [*Cowie et al.*, 1999]. Organic carbon concentrations in sediments on the Pakistan Margin (and elsewhere) are influenced by surface productivity, but also by dilution with lithogenic material, bottom-335 water oxygen (BWO) concentrations, bulk accumulation rate, sediment texture, and the mineral surface area [e.g.,*Paropkari et al.*, 1992; *Keil and Cowie*, 1999; *van der Weijden et al.*, 1999; *Suthhof et al.*,

2000]. We exclude an influence of BWO, because our core location coincides with the core depth of the OMZ where conditions have not varied significantly over the last 2400 years.

At our core site the use of TOC mass accumulation rates (TOC MAR) as a productivity indicator that theoretically remove an influence of dilution is complicated by strongly fluctuating sedimentation rates (SR ranging from 87 to 212 cm kyr^{-1}). Sediment mass accumulation rates (71 to 203 g cm^{-2} kyr^{-1}; event deposits excluded) calculated from SR and bulk densities are even higher than glacial/interglacial variations reported from the western (SR ranging from 6 to 38 cm kyr^{-1} and MAR ranging from 5 to 50 g cm^{-2} kyr^{-1} [*Emeis et al.*, 1995]) and eastern Arabian Sea (SR ranging from 4 to 9 cm kyr^{-1} [*Rostek et al.*, 1997]). SR and MAR at our study site are caused by highly variable input of lithogenic matter (range from 81 to 86%) from river runoff and/or dust storms [*Schulz et al.*, 1996; *von Rad et al.*, 1999]. Even though sedimentary OM in our core mainly consists of marine OM ($\delta^{13}C$ measured in core 275KL range from -21.5 to -19.5‰), significant positive correlations between TOC MAR and SR (R^2=0.56) and TOC MAR and sedimentary mass accumulation rates (R^2=0.76) indicate a dominant influence of bulk MAR (and thus alternating input of organic matter transported with mineral matter on its passage across the shelf) on organic carbon accumulation rates [*Müller and Suess*, 1979; *Emeis et al.* 1995]. This conclusion is supported by the good agreement between down-core variations in TOC MAR and varve thickness, which is an indicator for precipitation and river runoff [*von Rad et al.*, 1999; see Figure S1 in supporting information].

Over the last 2400 years of our record, elevated TOC concentrations coincide with increased $\delta^{15}N$ values and vice versa, a relationship described for Holocene sediments [*Agnihotri et al.*, 2003] and over glacial/interglacial cycles [*Altabet et al.*, 1995; *Ganeshram et al.*, 2000; *Suthhof et al.*, 2001] in the northern Indian Ocean. Parallel 361 changes in TOC concentrations and $\delta^{15}N$ are both related to productivity variations caused by variable access to the sub-thermocline nitrate pool. That nitrate pool has a high $\delta^{15}N$ resulting from denitrification within the upper part of the OMZ [*Gaye et al.*, 2013]. Upwelling does not occur at our core location, so that variable deepening of the mixed layer due to convective winter mixing during the NE monsoon season is the most likely process transporting the ^{15}N enriched nitrate to the ocean surface and enabling productivity. Together, $\delta^{15}N$ values and TOC concentrations in our sediment cores thus reflect productivity changes associated with mixed layer deepening due to NE monsoon conditions rather than variations in OMZ intensity. A third indirect signal of productivity is the ratio of the biogenic constituents carbonate (range from 6 to 15.5%) and opal (range from 0.5 to 0.9%), because high nutrient availability induces diatom blooms and high flux rates or organic matter, whereas high carbonate rain rates indicate low nutrient availability. The carbonate to opal ratio ranges from 14 to 29 and indicates a dominance of carbonate

primary producers (coccolithophores) at our study site that decreases over time relative to opal from diatoms [*Ramaswamy and Gaye*, 2006]. In this general trend, declining carbonate to opal ratios indicate a shift to higher productivity around 1400 A.D. (Fig. 4). All productivity parameters record periods of high productivity from 1400 to 1950 A.D. and periods of decreased productivity from about 200 B.C. to 250 A.D.

4.4. Variability in Sr/Ca ratios

The relationship between elevated Sr/Ca ratios and increased winter monsoon activity was first proposed for glacial/interglacial intervals by *Reichart et al.* [1998] and was later adapted for Holocene sediments by *Lückge et al.* [2001]. These authors proposed that elevated Sr/Ca ratios image variations in mixed layer depths: Because aragonite has a higher Sr content than calcite, variations in Sr/Ca track the depth interval of the aragonite compensation depth (ACD), and deepening of the ACD and higher Sr/Ca ratios indicate intensified 387 deep winter mixing due to elevated winter monsoon activity [*Reichart et al.*, 1998]. A different mechanism for changes in Sr/Ca on millennial time scales was proposed by *Böning and Bard* [2009], who attributed variations in Sr/Ca in the northeastern Arabian Sea to changes in the formation of Antarctic Intermediate Waters. For the 2400-year record here, this long-term variability is most likely irrelevant. The Sr/Ca ratio in the sediment cores vary between 0.023 and 0.032 at site 39KG/275KL (Fig. 5b), which is in the range of previously measured values for Holocene sediments from the Makran Area [*Lückge et al.*, 2001]. The increase in Sr/Ca ratios indicates a shift to winter monsoon conditions on the Pakistan Margin around 700 A.D.

5. Discussion

5.1. Local monsoon dynamics in the northeastern Arabian Sea during the last 2400 years

Winter monsoon activity affects both sea surface temperature and mixed layer depth over the Pakistan Margin, and thus controls the amount of thermocline nutrients entrained into the mixed layer. Our multi-proxy study from the northeastern Arabian Sea indicates four main periods of changing monsoon intensities throughout the late Holocene (Fig. 5). Summer monsoon intensity was high before about 250 A.D. and is recorded by high SSTs and generally low primary production due to diminished north-easterly winds and reduced convective winter mixing in the northeastern Arabian Sea. Summer monsoon intensity weakened (and winter monsoon mixing strengthened) after 250 A.D., which caused a cooling of the sea surface and slightly increased primary production. Finally, winter monsoon conditions started to predominate off Pakistan at about 700 A.D. as indicated by a shift to higher Sr/Ca ratios in core 275KL (Figure 5, note reverse Sr/Ca y-axis). While

winter monsoon intensity was still relatively weak between 700 and 1400 A.D., strong winter monsoon activity prevailed during the LIA from 1400 to 1900 A.D. as indicated by low SSTs and a peak in biological productivity due to strong convective winter 413 mixing. Low SSTs during the LIA as well as relatively high SSTs due to intensified SW monsoon conditions occurring 2000 years ago agree with another northeastern Arabian Sea (alkenone-based) SST reconstruction [*Doose-Rolinski et al.*, 2001]. Although both SST records differ in detail, possibly as a result of proxy uncertainty, they display similar trends of warming at around 0 A.D. and cooling during the LIA. This small-scale variability between both records might further be caused by the analysis of different core sections and thus variations in the time interval which is integrated by the alkenones.

The dynamics of the monsoon low-level wind system on the Pakistan Margin throughout the last 2400 years affect marine processes as well as moisture changes in this area. High salinity values before ~500 A.D. were caused by enhanced evaporation due to intense SW monsoon conditions, whereas variable but lower salinity after 500 A.D. probably reflects diminished SW monsoon and/or enhanced NE monsoon conditions [*Doose-Rolinski et al.*, 2001, see Figure 5]. *Lückge et al.* [2001] proposed a shift from SW monsoon dominated precipitation to NE monsoon precipitation in the Makran area around 500 A.D. These findings match our interpretation of predominating NE monsoon conditions since ~700 A.D.

Enhanced NE monsoonal activity during the LIA was most likely induced by an increased influence of Westerlies in the Makran area during this period. Today, winter rainfall brought by westerly winds and connected to cyclonic storms originating in the Mediterranean significantly contributes to total annual precipitation in the study area [*Lückge et al.*, 2001; *von Rad et al.*, 2002, and references therein]. Higher precipitation implicating stronger Westerlies on the coast off Pakistan after 1600 A.D. and during the LIA was deduced from varve thickness data from the nearby core SO90/56KG [*von Rad et al.,* 1999], and in a cave record from the Central Kumaun Himalaya [*Sanwal et al.*, 2013]. A significant feature preceding the LIA in the northeastern Arabian Sea is a distinct phase of increased SST (1050 to 1300 A.D.; see Figure 5) that coincides with the Medieval Warm Period 438 (MWP), a time of generally warm climate conditions observed in the Northern Hemisphere.

The response of the marine system to regional monsoon dynamics is best explained by reactions of the surface ocean to seasonal shifts in the ITCZ. The reversal of low level winds in the Arabian Sea during the seasonal cycle is accompanied by a shift in the location of the ITCZ. Core site 39KG/275KL is located at the average northern latitudinal position of the ITCZ, and thus surface ocean processes in this area are sensitive to long-term movements of the annual mean position of the ITCZ and the associate change in prevailing low-level winds. Northward migration of the ITCZ in

spring (SW monsoon) and southward retreat in autumn (NE monsoon) differentially impact on surface ocean salinity and temperature, and thus thermocline depth in the northeastern Arabian Sea. At times when the northern position of the ITCZ slightly shifts south of the average position, the duration of SW monsoon influence at site 275KL during summer is shortened. This would in turn enhance the influence of the winter monsoon on surface ocean conditions in this area.

We argue that long-term southward movement of the ITCZ throughout the late Holocene is responsible for the long-term trends of declining sea surface temperature and rising productivity seen in our record. Both reflect an increasing regional influence of the NE monsoon, and a reaction of the surface ocean by progressive winter deepening of convective mixing. This argument is supported by *Jung et al.* [2004] who attributed coherent basin wide decadal to century scale temperature variations in the Arabian Sea during the Holocene (based on a correlation between SST variations off Somalia and Pakistan) to a shift in the mean position of the ITCZ throughout the Holocene. Such a connection between a southward migrating annual mean position of the ITCZ and monsoon as well as precipitation changes throughout the Holocene was proposed by several authors [*Haug et al.*, 2001; *Lückge et al.*, 2001; *Fleitmann et al.*, 2003, 2007; *Russell and Johnson*, 2005; *Wang et al.*, 2005; *Yancheva et al.*, 2007; *Sinha et al.*, 2011]. Below we will discuss the see-saw of summer and winter monsoon activity around the long-term trend in the NE Arabian Sea record 464 that reflects

shorter-term variability of the regional climate system.

5.2. Reversed behaviour between summer and winter monsoon strength during the late Holocene

The mechanism above argues for an inverse relationship between summer and winter monsoon strength throughout the Indian and East Asian monsoon domain in the time-variant location of the ITCZ, expressed by decreasing summer monsoon intensity with increasing winter monsoon activity and vice versa [e.g., *Reichart et al.*, 2002; *Yancheva et al.*, 2007]. Is this inverse relationship evident in a comparison of our winter monsoon record with records of summer monsoon strength? The regions influenced most drastically by the SW monsoon are the Oman and the Somalia upwelling systems, that both registered a gradual warming of sea surface temperatures during the last 2400 years [*Huguet et al.,* 2006] in contrast to decreasing SST on the Pakistan Margin over this period. The same antagonistic behaviour is seen on centennial time scales and is most pronounced during the time intervals of greatest climate contrast over the last 2000 years on the Northern Hemisphere, namely the MWP (950 to 1250 A.D.) and the LIA (1400 to 1800 A.D.). Our conclusion was that winter monsoon strength off Pakistan was weak from 700 to 1400 A.D., contemporaneous with the

MWP. On the other hand, evidence for increased summer monsoon intensity during the MWP comes from the northwestern Arabian Sea [*Anderson et al.*, 2002, 2010; *Gupta et al.*, 2003], from Oman [*Fleitmann et al.*, 2004], India [*Sinha et al.*, 2007, 2011] as well as from China [*Zhang et al.*, 2008]. Most of these studies reconstructed diminished SW monsoon strength during the LIA, when our record suggests increased NE monsoon activity over the Pakistan Margin. Evidence of millennial trends and also on centennial time scales thus suggests that summer and winter monsoon strength was essentially anti-correlated over the late Holocene. During the last 400 years, however, SW monsoon strengthens 489 again in the northwestern Arabian Sea, probably as a result of a general warming trend [*Anderson et al.*, 2002]. Speleothem $\delta^{18}O$ from Kahf Defore in Southern Oman indicate summer monsoon rainfall generally above the long-term average since 1660 A.D. and support this hypothesis [*Fleitmann et al.*, 2004]. However, increasing SW monsoon intensity over the last 400 years is not recorded in the Pakistan Margin record, where winter monsoon indicators continue to dominate. Only most recently (since 1900 A.D.) primary productivity on the Pakistan Margin appear to decrease (as indicated by increased carbonate/opal ratios) and SSTs increase slightly, suggestive of intensified SW monsoon conditions in the northeastern Arabian Sea as well. The Oman cave record on land may be more sensitive to summer monsoon changes than the marine record in the Makran area, which is dominated by winter monsoon variability. Here, the direct response to climate may further be modulated by human activities: According to *Lückge et al.* [2012] reduction of river discharge and decreasing nutrient supply due to building of dams and irrigation facilities may be the reason for the observed decline in productivity during the last 100 years in the northeastern Arabian Sea. The antagonism of SW and NE monsoon influence is evident in our record and agrees with other monsoon reconstructions in the Arabian Sea and beyond. Based on the assumption that the $\delta^{18}O$-signal measured in speleothems from Wanxiang Cave is mainly influenced by summer monsoon precipitation, *Zhang et al.* [2008] compiled a 1810-year long record of summer monsoon intensity for central China. Their $\delta^{18}O$ variations show a strong resemblance to our reconstructed SST-curve with lower SST in the northeastern Arabian Sea coinciding with a decline in summer monsoon rainfall in central China due to weaker East Asian summer monsoon intensity (Figure 6). Furthermore, SST variations in the northeastern Arabian Sea are not only related to changes in East Asian summer monsoon over central China, but also to changes in SSTs from the Indo-Pacific warm pool [*Oppo et al.*, 2009, Figure 6]. In accordance with our interpretation, *Oppo et al.* [2009] suggested that strong sea surface cooling in the Markassar Strait during the LIA was caused by 515 intensified winter monsoon conditions rather than by monsoon induced upwelling. We thus conclude that a linkage between summer and winter monsoon strength exists over the whole

Asian monsoon system during the late Holocene, reflecting long-term and short-term shifts in the ITCZ.

5.3. Global connections: The LIA climate feature

The monsoon record from the Pakistan Margin is in phase with characteristic, northern hemispheric climate periods of the late Holocene, such as the Little Ice Age, the MedievalWarm Period and the Roman Warm Period (RWP). It reveals a consistent pattern of increased summer monsoon activity in the northeastern Arabian Sea during northern hemispheric warm periods (MWP, RWP) and strengthened winter monsoon activity during hemispheric colder periods (LIA). Our high-resolution record implies that this consistent link between the North Atlantic and the Indian Ocean, which was described for glacial/interglacial [e.g., *Sirocko et al.*, 1993; *Schulz et al.*, 1998; *Schulte and Müller*, 2001] to climatological [*Gupta et al.*, 2003] time scales, appears to operate during historical times as well. It causes the SW monsoon to weaken and the NE monsoon to gain strength during colder climate conditions over the North Atlantic. One of the most prominent climate features in the northeastern Arabian Sea over the last 2400 years was the sharp decrease in SST due to strengthening NE monsoon conditions between 1400 and 1850 A.D., contemporaneous with the LIA. Once described as a climate period restricted only to the northern extratropical Hemisphere [e.g., *Keigwin*, 1996], LIA climate conditions appear to have impacted on SST in low latitude regions as well [*DeMenocal*, 2000; *Black et al.*, 2007; *Oppo et al.*, 2009]. A recently published global data set of proxy records indeed confirms a global cooling trend between 1580 and 1880 A.D. [*PAGES 2k Consortium*, 2013] that is preceded by a phase of low solar irradiance between 1450 to 1750 A.D. [*Bard et al.*, 2000], suggesting that LIA climate conditions may at least partly be influenced by solar forcing. Solar radiation has been proposed 541 as a forcing mechanism controlling both North Atlantic climate [*Bond et al.*, 2001] as well as variations in monsoon intensity during the Holocene [*Neff et al.*, 2001; *Agnihotri et al.*, 2002; *Fleitmann et al.*, 2003; *Gupta*, 2005; *Wang et al.*, 2005]. We thus infer that the decline in SST and increased NE monsoonal wind strength in the northeastern Arabian Sea during the LIA were triggered by generally colder climate conditions due to low solar insolation.

6. Conclusions

Our high-resolution reconstruction of primary productivity and alkenone-derived SST from the northeastern Arabian Sea provides a unique record of winter monsoon variability throughout the late Holocene. In this area, primary production and sea surface temperatures are linked to winter monsoon intensity that cools the sea surface and increases its salinity so that thermocline deepening

entrains more nutrients into the mixed layer and raises. productivity. Because core 275KL is located in a sensitive region at the modern northern mean latitudinal position of the ITCZ, observed changes in surface ocean properties in response to the monsoonal wind regime on the Pakistan Margin track long-term and short557 term movements of the ITCZ throughout the late Holocene. Reconstructed SST decreased whereas productivity increased over the last 2400 years, imaging a long-term trend of NE monsoon strengthening in response to insolation-induced southward migration of the ITCZ. Comparison of our winter monsoon record with records of summer monsoon intensity confirms an antagonistic relationship between summer and winter monsoon strength during the last 2400 years that holds also for centennial climate variations. Reconstructed monsoon variability supports the growing body of evidence that significant climate variability occurs not only on timescales of several hundred of thousand years but also through the late Holocene. Before 700 A.D. winter monsoon activity in the northeastern Arabian Sea was generally weak and convective winter mixing was shallow, indicated by high SSTs (~ 28.3°C) and reduced primary productivity. 567 Winter monsoon conditions started to predominate off Pakistan at about 700 A.D. in response to the overall southward movement of average ITCZ location during the late Holocene. While winter monsoon activity was weak during the MWP from 700 to 1400 A.D., strong sea surface cooling down to 26.9°C and a peak in primary productivity indicated strong and prevailing winter monsoon activity during the LIA from 1400 to 1900 A.D. The coherence between monsoon-induced variations over the Pakistan Margin with other monsoon records indicates a strong linkage of climate variability in the entire Asian monsoon system during the late Holocene, caused by migration of the ITCZ.

Acknowledgments

We thank S. Beckmann and F. Langenberg for analytical support. Financial support was provided by the German Federal Ministry of Education and Research (BMBF) grant No.1 03G0806B (CARIMA) and is gratefully acknowledged. This is NIO contribution No.XXXX

References

Agnihotri, R., K. Dutta, R. Bhushan, and B. L. K. Somayajulu (2002), Evidence for solar forcing on the Indian monsoon during the last millennium, *Earth and Planetary Science Letters*, *198*, 521-527.

Agnihotri, R., S. K. Bhattacharya, M. M. Sarin, and B. L. K. Somayajulu (2003), Changes in surface productivity and subsurface denitrification during the Holocene: a multiproxy study from the eastern Arabian Sea, *The Holocene*, *13*, 701-713, doi:10.1191/0959683603hl656rp.

Agnihotri, R., S. Kurian, M. Fernandes, K. Reshma, W. D'Souza, and S. W. A. Naqvi (2008), Variability of subsurface denitrification and surface productivity in the coastal eastern Arabian Sea over the past seven centuries, *The Holocene*, *18*, 755-764, doi:10.1177/0959683608091795.

Altabet, A., D. W. Murray, and W. L. Prell (1999), Climatically linked oscillation in Arabian Sea denitrification over the past 1 m.y.: Implications for the marine N cycle, *Paleoceanography*, *14*(6), 732-743.

Altabet, M. A., R. Francois, D. W. Murray, and W. L. Prell (1995), Climate-related variations in denitrification in the Arabian Sea from sediment $^{15}N/^{14}N$ ratios, *Nature*, *373*, 506-509.

Anderson, D. M., J. T. Overpeck, and A. K. Gupta (2002), Increase in the Asian Southwest Monsoon during the past Four Centuries, *Science*, *297*(5581), 596-599.

Anderson, D. M., C. K. Baulcomb, A. K. Duvivier, and A. K. Gupta (2010), Indian summer monsoon during the last two millennia, *Journal of Quaternary Science*, *25*(6), 911-917, doi:10.1002/jqs.1369.

Andruleit, H. A., U. von Rad, A. Bruns, and V. Ittekkot (2000), Coccolithophore fluxes from sediment traps in the northeastern Arabian Sea off Pakistan, *Marine Micropaleontology*, *38*, 285-308.

Banse, K., and C. R. McClain (1986), Winter blooms of phytoplankton in the Arabian Sea as observed by the Coastal Zone Color Scanner, *Marine Ecology - Progress Series*, *34*, 201-211.

Bard, E., G. Raisbeck, F. Yiou, and J. Jouzel (2000), Solar irradiance during the last 1200 years based on cosmogenic nuclides, *Tellus*, *52B*, 985-992, doi:10.1034/j.1600-0889.2000.d01-7.x.

Berkelhammer, M., A. Sinha, M. Mudelsee, H. Cheng, R. L. Edwards, and K. G. Cannariato (2010), Persistent multidecadal power of the Indian Summer Monsoon, *Earth and Planetary Science Letters*, *290*, 166-172, doi:doi:10.1016/j.epsl.2009.12.017.

Black, D. E., M. a. Abahazi, R. C. Thunell, A. Kaplan, E. J. Tappa, and L. C. Peterson (2007), An 8-century tropical Atlantic SST record from the Cariaco Basin: Baseline variability, twentieth-century warming, and Atlantic hurricane frequency, *Paleoceanography*, *22*, doi:10.1029/2007PA001427.

Bond, G., W. Showers, M. Cheseby, R. Lotti, P. Almasi, P. DeMenocal, P. Priore, H. Cullen, I. Hajdas, and G. Bonani (1997), A Pervasive Millennial-Scale Cycle in North Atlantic Holocene and Glacial Climates, *Science*, *278*, 1257-1266, doi:10.1126/science.278.5341.1257.

Bond, G., B. Kromer, J. Beer, R. Muscheler, M. N. Evans, W. Showers, S. Hoffmann, R. Lotti-Bond, I. Hajdas, and G. Bonani (2001), Persistent Solar Influence on North Atlantic Climate During the Holocene., *Science*, *294*, 2130-2136, doi:10.1126/science.1065680.

Brand, T. D., and C. Griffiths (2009), Seasonality in the hydrography and biogeochemistry across the Pakistan margin of the NE Arabian Sea, *Deep Sea Research II*, *56*, 283-295, doi:10.1016/j.dsr2.2008.05.036.

Brassell, S. C., G. Eglinton, I. T. Marlowe, U. Pflaumann, and M. Sarnthein (1986), Molecular stratigraphy: a new tool for climate assessment, *Nature*, *320*, 129-133.

Broerse, A. T. C., G.-J. A. Brummer, and J. E. Van Hinte (2000), Coccolithophore export production in response to monsoonal upwelling off Somalia (northwestern Indian Ocean), *Deep Sea Research II*, *47*, 2179-2205, doi:10.1016/S0967-0645(00)00021-7.

Burns, S. J., D. Fleitmann, M. Mudelsee, U. Neff, A. Matter, and A. Mangini (2002), A 780-year annually resolved record of Indian Ocean monsoon precipitation from a speleothem from south Oman, *Journal of Geophysical Research*, *107*, doi:10.1029/2001JD001281.

Chauhan, O. S., E. Vogelsang, N. Basavaiah, and U. S. A. Kader (2010), Reconstruction of the variability of the southwest monsoon during the past 3 ka, from the continental margin of the southeastern Arabian Sea, *Journal Of Quaternary Science*, *25*(5), 798-807.

Clemens, S., W. L. Prell, D. W. Murray, G. Shimmield, and G. Weedon (1991), Forcing mechanisms of the Indian Ocean monsoon, *Nature*, *353*, 720-725.

Conley, D. J. (1998), An interlaboratory comparison for the measurement of biogenic silica in sediments, *Marine Chemistry*, *63*, 39-48, doi:10.1016/S0304-4203(98)00049-8.

Conte, M. H., G. Eglinton, and L. A. S. Madureira (1992), Long-chain alkenones and alkyl alkenoates as palaeotemperature indicators: their production, flux and early sedimentary diagenesis in the Eastern North Atlantic, *Advances in Organic Geochemistry 1991*, *19*, 287-298, doi:10.1016/0146-6380(92)90044-X.

Conte, M. H., M.-A. Sicre, C. Rühlemann, J. C. Weber, S. Schulte, D. Schulz-Bull, and T. Blanz (2006), Global temperature calibration of the alkenone unsaturation index ($U^{K'}_{37}$) in surface waters and comparison with surface sediments, *Geochemistry, Geophysics, Geosystems*, *7*(2), doi:10.1029/2005GC001054.

Cowie, G. L., S. E. Calvert, T. F. Pedersen, H. Schulz, and U. Rad (1999), Organic content and preservational controls in surficial shelf and slope sediments from the Arabian Sea (Pakistan margin), *Marine Geology*, *161*, 23-38.

Dahl, K. A., and D. W. Oppo (2006), Sea surface temperature pattern reconstructions in the Arabian Sea, *Paleoceanography*, *21*, doi:10.1029/2005PA001162.

DeMaster, D. J. (1981), The supply and accumulation of silica in the marine environment, *Geochimica et Cosmochimica Acta*, *45*, 1715-1732, doi:10.1016/0016-7037(81)90006-5.

DeMenocal, P. (2000), Coherent High- and Low-Latitude Climate Variability During the Holocene Warm Period, *Science*, *288*, 2198-2202, doi:10.1126/science.288.5474.2198.

Doose-Rolinski, H., U. Rogalla, G. Scheeder, A. Lückge, and U. von Rad (2001), High-resolution temperature and evaporation changes during the late Holocene in the northeastern Arabian Sea, *Paleoceanography*, *16*(4), 358-367.

Fleitmann, D., S. J. Burns, M. Mudelsee, U. Neff, J. Kramers, A. Mangini, and A. Matter (2003), Holocene Forcing of Indian Monsoon Recorded in a Stalagmite from Southern Oman, *Science*, *300*(5626), 1737-1739.

Fleitmann, D., S. J. Burns, U. Neff, M. Mudelsee, A. Mangini, and A. Matter (2004), Palaeoclimatic interpretation of high-resolution oxygen isotope profiles derived from annually laminated speleothems from Southern Oman, *Quaternary Science Reviews*, *23*, 935-945.

Fleitmann, D. et al. (2007), Holocene ITCZ and Indian monsoon dynamics recorded in stalagmites from Oman and Yemen (Socotra), *Quaternary Science Reviews*, *26*, 170-188, doi:10.1016/j.quascirev.2006.04.012.

Ganeshram, S., F. Pedersen, E. Calvert, W. McNeill, and M. R. Fontugne (2000), Glacial-interglacial variability in denitrification in the world's oceans: Causes and consequences, *Paleoceanography*, *15*(4), 361-376.

Gaye, B., B. Nagel, K. Dähnke, T. Rixen, and K.-C. Emeis (2013), Evidence of parallel denitrification and nitrite oxidation in the ODZ of the Arabian Sea from paired stable isotopes of nitrate and nitrite, *Global Biogeochemical Cycles*, doi:10.1002/2011GB004115

Gupta, A. K., D. M. Anderson, and J. T. Overpeck (2003), Abrupt changes in the Asian southwest monsoon during the Holocene and their links to the North Atlantic Ocean, *Nature*, *421*, 354-356.

Haake, B., V. Ittekkot, T. Rixen, V. Ramaswamy, R. R. Nair, and W. B. Curry (1993), Seasonality and interannual variability of particle fluxes to the deep Arabian sea, *Deep Sea Research I*, *40*, 1323-1344.

Hastenrath, S., and P. J. Lamb (1979), *Climate Atlas of the Indian Ocean, vol.1, Surface Climate and Atmospheric Circulation*, University of Wisconsin Press, Madison.

Haug, G. H., K. A. Hughen, D. M. Sigman, L. C. Peterson, and U. Röhl (2001), Southward migration of the intertropical convergence zone through the Holocene, *Science*, *293*, 1304-1308, doi:10.1126/science.1059725.

Hong, Y. T. et al. (2003), Correlation between Indian Ocean summer monsoon and North Atlantic climate during the Holocene, *Earth and Planetary Science Letters*, *211*, 371-380.

Huguet, C., J.-H. Kim, J. S. Sinninghe Damsté, and S. Schouten (2006), Reconstruction of sea surface temperature variations in the Arabian Sea over the last 23 kyr using organic proxies (TEX_{86} and $U^{K'}_{37}$), *Paleoceanography*, *21*, PA3003, doi:10.1029/2005PA001215.

Jung, S. J. A., G. R. Davies, G. Ganssen, and D. Kroon (2004), Synchronous Holocene sea surface temperature and rainfall variations in the Asian monsoon system, *Quaternary Science Reviews*, *23*, 2207-2218.

Keigwin, L. D. (1996), The Little Ice Age and Medieval Warm Period in the Sargasso Sea, *Science*, *274*, 1504-1508.

Levitus, S., and T. Boyer (1994), *World Ocean Atlas 1994*, vol. 4, *Temperature, NOAA Atlas NESDIS*, vol. 4, U.S. department of Commerce, Washington, D.C.

Lückge, A., H. Doose-Rolinski, A. A. Khan, H. Schulz, and U. von Rad (2001), Monsoonal variability in the northeastern Arabian Sea during the past 5000 years: geochemical evidence from laminated sediments, *Palaeogeography, Palaeoclimatology, Palaeoecology*, *167*, 273-286.

Lückge, A., G. Deplazes, H. Schulz, G. Scheeder, A. Suckow, S. Kasten, and G. H. Haug (2012), Impact of Indus River discharge on productivity and preservation of organic carbon in the Arabian Sea over the twentieth century, *Geology*, *40*(5), 399-402, doi:10.1130/G32608.1.

Madhupratap, M., S. Prasanna Kumar, P. M. A. Bhattathiri, M. Dileep Kumar, S. Raghukumar, K. K. C. Nair, and N. Ramaiah (1996), Mechanism of the biological response to winter cooling in the northeastern Arabian Sea, *Nature*, *384*, 549-552.

Madureira, L. A. S., M. H. Conte, and G. Eglinton (1995), Early diagenesis of lipid biomarker compounds in North Atlantic sediments, *Paleoceanography*, *10*(3), 627-642.

Mann, M. E., Z. Zhang, S. Rutherford, R. S. Bradley, M. K. Hughes, D. Shindell, C. Ammann, G. Faluvegi, and F. Ni (2009), Global Signatures and Dynamical Origins of the Little Ice Age and Medieval Climate Anomaly, *Science*, *326*, 1256-1260, doi:10.1126/science.1177303.

Müller, P., G. Kirst, G. Ruhland, I. von Storch, and A. Rosell-Melé (1998), Calibration of the alkenone paleotemperature index $U^{K'}_{37}$ based on core-tops from the eastern South Atlantic and the global ocean (60°N-60°S), *Geochimica et Cosmochimica Acta*, *62*(10), 1757-1772.

Nair, R. R., V. Ittekkot, S. J. Manganini, V. Ramaswamy, B. Haake, E. T. Degens, B. N. Desai, and S. Honjo (1989), Increased particle flux to the deep ocean related to monsoons, *Nature*, *338*, 749-751.

Naqvi, S. W. A., T. Yoshinari, D. A. Jayakumar, M. A. Altabet, P. V. Narvekar, A. H. Devol, J. A. Brandes, and L. A. Codispoti (1998), Budgetary and biogeochemical implications of N_2O isotope signatures in the Arabian Sea, *Nature*, *394*, 462-464.

Neff, U., S. J. Burns, A. Mangini, M. Mudelsee, D. Fleitmann, and A. Matter (2001), Strong coherence between solar variability and the monsoon in Oman between 9 and 6 kyr ago., *Nature*, *411*, 290-293, doi:10.1038/35077048.

Olson, D. B., G. L. Hitchcock, R. A. Fine, and B. A. Warren (1993), Maintenance of the low-oxygen layer in the central Arabian Sea, *Deep Sea Research II*, *40*(3), 673-685.

Oppo, D. W., Y. Rosenthal, and B. K. Linsley (2009), 2,000-year-long temperature and hydrology reconstructions from the Indo-Pacific warm pool, *Nature*, *460*, 1113-1116, doi:10.1038/nature08233.

PAGES 2k Consortium (2013), Continental-scale temperature variability during the past two millennia, *Nature Geoscience*, *6*, 339-346, doi:10.1038/NGEO1797.

Paropkari, A. L., C. P. Babu, and A. Mascarenhas (1992), A critical evaluation of depositional parameters controlling the variability of organic carbon in Arabian Sea sediments, *Marine Geology*, *107*, 213-226.

Prahl, F. G., G. J. de Lange, M. Lyle, and M. A. Sparrow (1989), Post-depositional stability of long-chain alkenones under contrasting redox conditions, *Nature*, *341*, 434-437.

Prahl, F. G., J. Dymond, and M. a Sparrow (2000), Annual biomarker record for export production in the central Arabian Sea, *Deep Sea Research Part II*, *47*, 1581-1604, doi:10.1016/S0967-0645(99)00155-1.

Prasanna Kumar, S., and T. G. Prasad (1996), Winter cooling in the northern Arabian Sea, *Current Science*, *71*(10), 834-841.

Prasanna Kumar, S., N. Ramaiah, M. Gauns, V. V. S. S. Sarma, P. M. Muraleedharan, S. Raghukumar, M. Dileep Kumar, and M. Madhupratap (2001), Physical forcing of biological productivity in the Northern Arabian Sea during the Northeast Monsoon, *Deep Sea Research Part II*, *48*, 1115-1126, doi:10.1016/S0967-0645(00)00133-8.

von Rad, U., H. Schulz, and SONNE 90 Scientific Party (1995), Sampling the oxygen minimum zone off Pakistan: glacial-interglacial variations of anoxia and productivity (preliminary results, SONNE 90 cruise), *Marine Geology*, *125*, 7-19.

von Rad, U., M. Schaaf, K. H. Michels, H. Schulz, W. H. Berger, and F. Sirocko (1999), A 5000-yr Record of Climate Change in Varved Sediments from the Oxygen Minimum Zone off Pakistan, Northeastern Arabian Sea, *Quaternary Research*, *51*, 39-53.

von Rad, U., A. A. Khan, W. H. Berger, D. Rammlmair, and U. Treppke (2002), Varves, turbidites and cycles in upper Holocene sediments (Makran slope, northern Arabian Sea), *Geological Society, London, Special Publications*, *195*, 387-406.

Ramaswamy, V., and B. Gaye (2006), Regional variations in the fluxes of foraminifera carbonate, coccolithophorid carbonate and biogenic opal in the northern Indian Ocean, *Deep Sea Research I*, *53*, 271-293, doi:10.1016/j.dsr.2005.11.003.

Van Rampelbergh, M. et al. (2013), Mid- to late Holocene Indian Ocean Monsoon variability recorded in four speleothems from Socotra Island, Yemen, *Quaternary Science Reviews*, *65*, 129-142, doi:10.1016/j.quascirev.2013.01.016.

Reichart, G. J., L. J. Lourens, and W. J. Zachariasse (1998), Temporal variability in the northern Arabian Sea Oxygen Minimum Zone (OMZ) during the last 225,000 years, *Paleoceanography*, *13*(6), 607-621.

Reichart, G. J., S. J. Schenau, G. J. de Lange, and W. J. Zachariasse (2002), Synchroneity of oxygen minimum zone intensity on the Oman and Pakistan Margins at sub-Milankovitch time scales, *Marine Geology*, *185*, 403-415, doi:10.1016/S0025-3227(02)00184-6.

Reynolds, R. W., N. A. Rayner, T. M. Smith, D. C. Stokes, and W. Wang (2002), An Improved In Situ and Satellite SST Analysis for Climate, *Journal of Climate*, *15*, 1609-1625.

Rontani, J.-F., J. K. Volkman, F. G. Prahl, and S. G. Wakeham (2013), Biotic and abiotic degradation of alkenones and implications for paleoproxy applications: A review, *Organic Geochemistry*, doi:10.1016/j.orggeochem.2013.04.005.

Rosell-Melé, A., and F. G. Prahl (2013), Seasonality of $U^{K'}_{37}$ temperature estimates as inferred from sediment trap data, *Quaternary Science Reviews*, *72*, 128-136, doi:10.1016/j.quascirev.2013.04.017.

Rostek, F., E. Bard, L. Beaufort, C. Sonzogni, and G. Ganssen (1997), Sea surface temperature and productivity records for the past 240 kyr in the Arabian Sea, *Deep Sea Research II*, *44*(6-7), 1461-1480.

Russell, J. M., and T. C. Johnson (2005), Late Holocene climate change in the North Atlantic and equatorial Africa: Millennial-scale ITCZ migration, *Geophysical Research Letters*, *32*, L17705, doi:10.1029/2005GL023295.

Sanwal, J., B. S. Kotlia, C. Rajendran, S. M. Ahmad, K. Rajendran, and M. Sandiford (2013), Climatic variability in Central Indian Himalaya during the last 1800 years: Evidence from a high resolution speleothem record, *Quaternary International*, doi:10.1016/j.quaint.2013.03.029.

Schlitzer, R. (2013), Ocean Data View, http://odv.awi-bremerhaven.de

Schulte, S., and P. Müller (2001), Variations of sea surface temperature and primary productivity during Heinrich and Dansgaard-Oeschger events in the northeastern Arabian Sea, *Geo-Marine Letters*, *21*, 168-175, doi:10.1007/s003670100080.

Schulte, S., F. Rostek, E. Bard, J. Rullkötter, and O. Marchal (1999), Variations of oxygen-minimum and primary productivity recorded in sediments of the Arabian Sea, *Earth and Planetary Science Letters*, *173*, 205-221, doi:10.1016/S0012-821X(99)00232-0.

Schulz, H., U. Von Rad, and U. Von Stackelberg (1996), Laminated sediments from the oxygen-minimum zone of the northeastern Arabian Sea, *Geological Society, London, Special Publications*, *116*, 185-207, doi:10.1144/GSL.SP.1996.116.01.16.

Schulz, H., U. von Rad, and H. Erlenkeuser (1998), Correlation between Arabian Sea and Greenland climate oscillations of the past 110,000 years, *Nature*, *393*, 54-57.

Schulz, H., U. von Rad, and V. Ittekkot (2002), Planktic foraminifera, particle flux and oceanic productivity off Pakistan, NE Arabian Sea: modern analogues and application to the palaeoclimatic record, *Geological Society, London, Special Publications*, *195*, 499-516, doi:10.1144/GSL.SP.2002.195.01.27.

Sikes, E. L., J. W. Farrington, and L. D. Keigwin (1991), Use of the alkenone unsaturation ratio $U^{K'}_{37}$ to determine past sea surface temperatures: core-top SST calibrations and methodology considerations, *Earth and Planetary Science Letters*, *104*, 36-47.

Sinha, A., K. G. Cannariato, L. D. Stott, H. Cheng, R. L. Edwards, M. G. Yadava, R. Ramesh, and I. B. Singh (2007), A 900-year (600 to 1500 A.D.) record of the Indian summer monsoon precipitation from the core monsoon zone of India, *Geophysical Research Letters*, *34*, doi:10.1029/2007GL030431.

Sinha, A., L. D. Stott, M. Berkelhammer, H. Cheng, R. L. Edwards, B. Buckley, M. Aldenderfer, and M. Mudelsee (2011), A global context of megadroughts in monsoon Asia during the past millennium, *Quaternary Science Reviews*, *30*, 47-62.

Sirocko, F., M. Sarnthein, H. Erlenkeuser, H. Lange, M. Arnold, and J. C. Duplessy (1993), Century-scale events in monsoonal climate over the past 24,000 years, *Nature*, *364*, 322-324.

Sonzogni, C., E. Bard, F. Rostek, R. Lafont, A. Rosell-Mele, and G. Eglinton (1997a), Core-top calibrations of the alkenone index vs sea surface temperature in the Indian Ocean, *Deep Sea Research II*, *44*(6-7), 1445-1460.

Sonzogni, C., E. Bard, F. Rostek, D. Dollfus, A. Rosell-Melé, and G. Eglinton (1997b), Temperature and Salinity Effects on Alkenone Ratios Measured in Surface Sediments from the Indian Ocean, *Quaternary Research*, *47*, 344-355.

Suthhof, A., T. C. Jennerjahn, P. Schäfer, and V. Ittekkot (2000), Nature of organic matter in surface sediments from the Pakistan continental margin and the deep Arabian Sea: amino acids, *Deep-Sea Research II*, *47*, 329-351.

Suthhof, A., V. Ittekkot, and B. Gaye-Haake (2001), Millennial-scale oscillation of denitrification intensity in the Arabian Sea during the late Quaternary and its potential influence on atmospheric N_2O and global climate, *Global Biogeochemical Cycles*, *0*, 1-13.

Wakeham, S. G., M. L. Peterson, J. I. Hedges, and C. Lee (2002), Lipid biomarker fluxes in the Arabian Sea, with a comparison to the equatorial Pacific Ocean, *Deep Sea Research II*, *49*, 2265-2301, doi:10.1016/S0967-0645(02)00037-1.

Wang, Y., H. Cheng, R. L. Edwards, Y. He, X. Kong, Z. An, J. Wu, M. J. Kelly, C. A. Dykoski, and X. Li (2005), The Holocene Asian Monsoon: Links to Solar Changes and North Atlantic Climate, *Science*, *308*, 854-857, doi:10.1126/science.1106296.

Wyrtki, K. (1973), Physical Oceanography of the Indian Ocean, in *The Biology of the Indian Ocean*, edited by B. Zeitzschel, pp. 18-36, Springer, Berlin.

Yancheva, G., N. R. Nowaczyk, J. Mingram, P. Dulski, G. Schettler, J. F. W. Negendank, J. Liu, D. M. Sigman, L. C. Peterson, and G. H. Haug (2007), Influence of the intertropical convergence zone on the East Asian monsoon., *Nature*, *445*, 74-77, doi:10.1038/nature05431.

Zhang, P. et al. (2008), A Test of Climate, Sun, and Culture Relationships from an 1810-Year Chinese Cave Record, *Science*, *322*, 940-942.

Figure Captions

Figure1

Study area in the northeastern Arabian Sea off Pakistan with core locations 275KL and 39KG and sediment trap station EPT-2. Shaded area indicates OMZ impinging on the continental slope. Bathymetry is shown in meters. Inset: Vertical profile of core 275KL showing varve-like lamination. This map is produced by using Ocean Data View [*Schlitzer*, 2013].

Figure 2

Annual variability of mixed layer depth and SST for site 275KL extracted from the World Ocean Atlas [*Levitus and Boyer*, 1994] and total particle flux measured in sediment trap EPT-2 after *Andruleit et al.* [2000]. Increased particle fluxes occur during the NE monsoon season when strong convective winter mixing deepens the mixed layer and SST decreases.

Figure 3

(A) Total coccolith [*Andruleit et al.*, 2000] and alkenone fluxes at trap EPT-2 in the northeastern Arabian Sea off Pakistan. (B) Alkenone-derived SST measured in EPT-2 samples (triangle) compared to 1995/1996 monthly SST (circle; extracted from the web-site http://ingrid.ldgo.columbia.edu). Mean alkenone SST is about 0.4°C higher than mean temperature over May 1995 to February 1996.

Figure 4

Late Holocene alkenone SST (bold line: running mean of 3) and productivity record for cores 39KG and 275KL from the northeastern Arabian Sea. Carbonate/opal ratios, $\delta^{15}N$ values (bold line: running mean of 3) and smoothed TOC contents (running average of 11) were used as productivity indicators. Dashed lines indicate the respective mean over the complete dataset. Further illustrated are characteristic climate periods known from the northern Hemisphere: Little Ice Age (LIA); Medieval Warm Period (MWP); Cold Dark Ages (CDA) and Roman Warm Period (RWP).

Figure 5

Reconstruction of monsoonal variability in the northeastern Arabian Sea during the last 2400 years. Alkenone SST record (bold line: 3-point running mean) and smoothed Sr/Ca ratios (21-point running mean) for core 39KG/275KL compared to reconstructed salinity variations in core 39KG/56KA for the northeastern Arabian Sea from *Doose-Rolinski et al.* [2001]. Dashed lines indicate the respective mean over the studied time interval.

Figure 6

(A) Late Holocene alkenone-derived SST variations (cores 39KG and 275KL) from the northeastern Arabian Sea compared to (B) Mg/Ca SST variations reconstructed for the Markassar Strait (Indonesia) by *Oppo et al.* [2009] and (C) a smoothed $\delta^{18}O$ record (15-point moving average) of Wanxiang Cave (China) as an indicator for summer monsoon intensity from *Zhang et al.* [2008]. Dashed lines indicate the respective mean over the studied time interval.

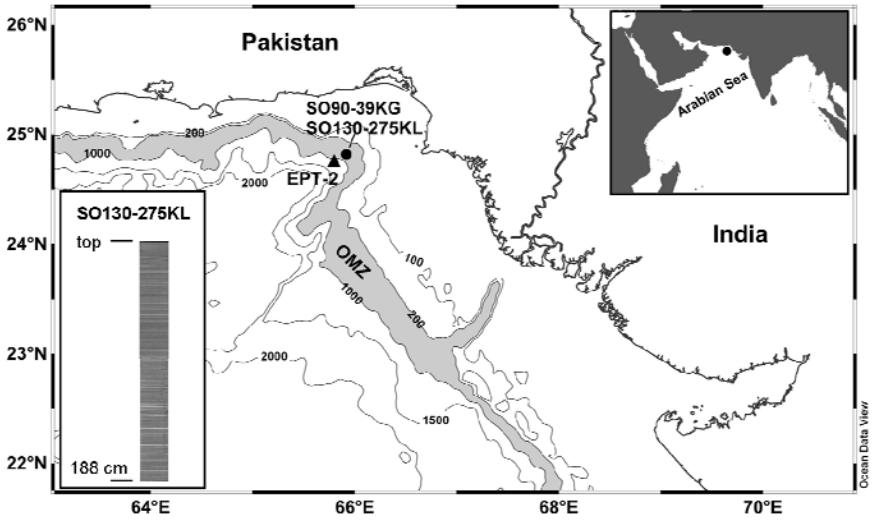

Figure 1

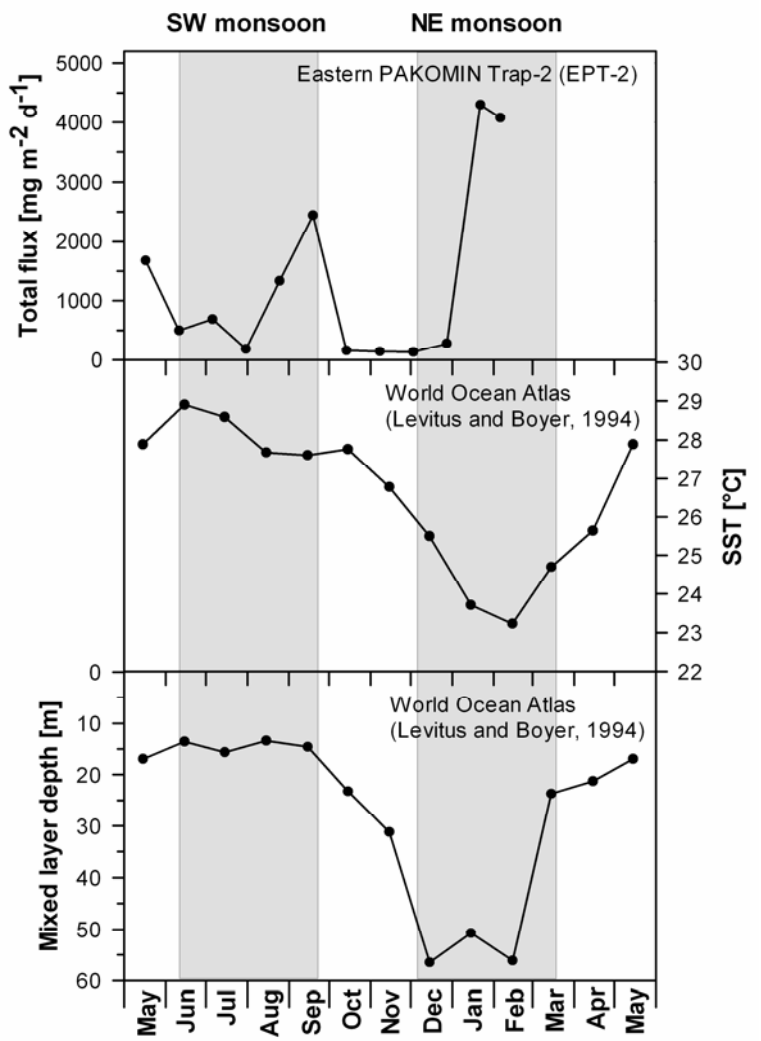

Figure 2

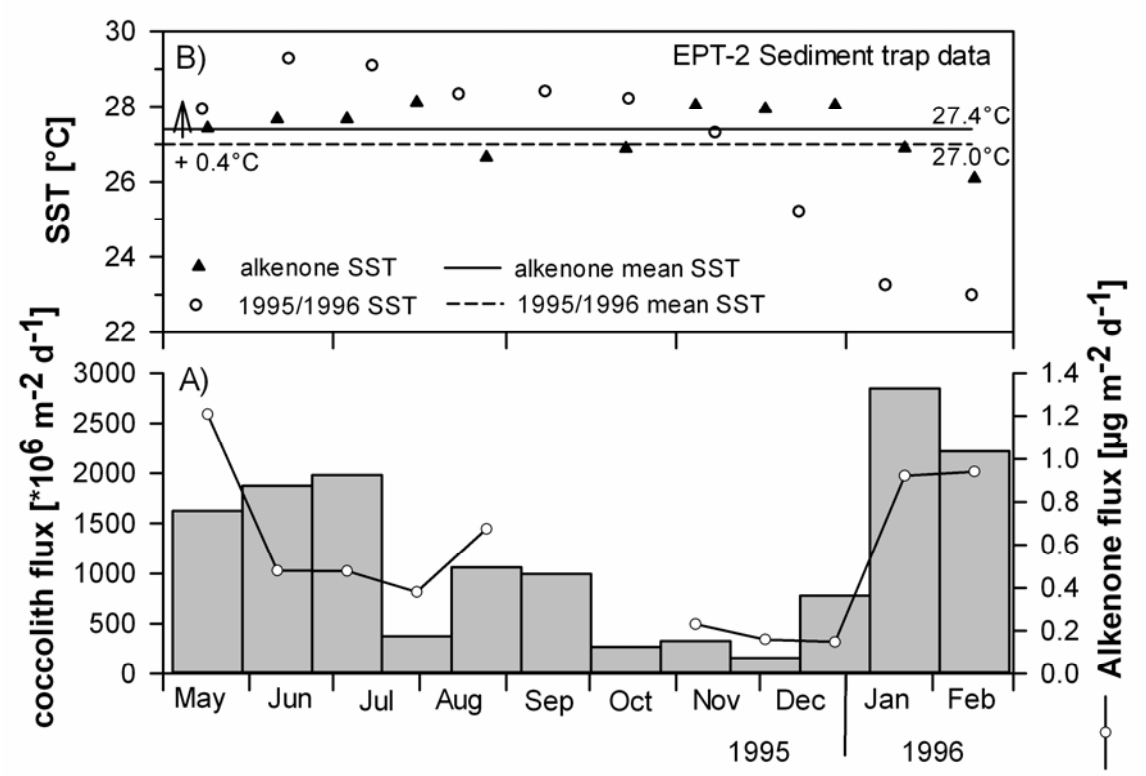
B)
EPT-2 Sediment trap data
SST [°C]
30
28
26
24
22
27.4°C
27.0°C
+ 0.4°C
alkenone SST
alkenone mean SST
1995/1996 SST
1995/1996 mean SST
A)
coccolith flux [*10^6 m^-2 d^-1]
Alkenone flux [µg m^-2 d^-1]
3000
2500
2000
1500
1000
500
0
1.4
1.2
1.0
0.8
0.6
0.4
0.2
0.0
May
Jun
Jul
Aug
Sep
Oct
Nov
Dec
Jan
Feb
1995
1996

Figure 3

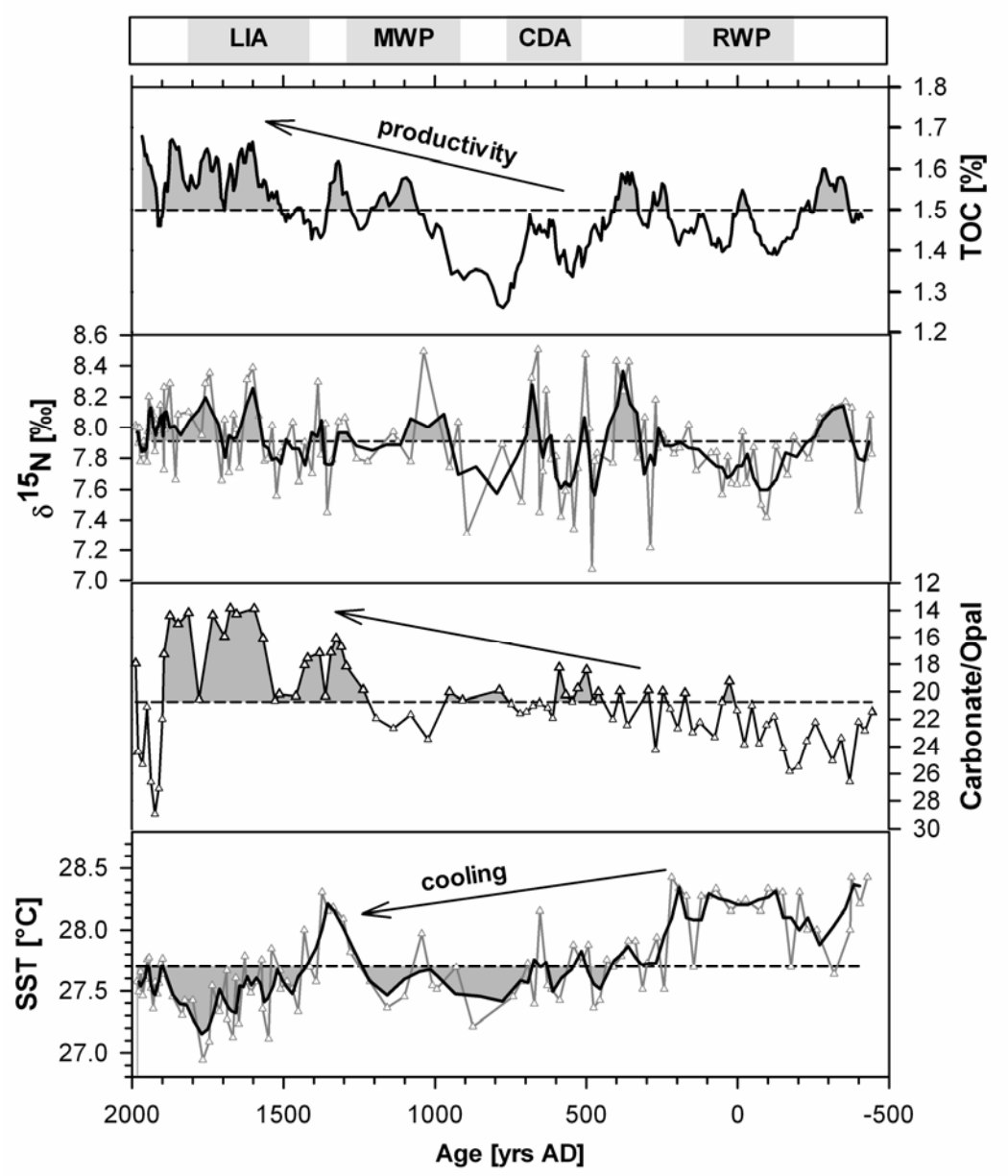
LIA
MWP
CDA
RWP
productivity
TOC [%]
δ15N [‰]
Carbonate/Opal
cooling
SST [°C]
Age [yrs AD]

Figure 4

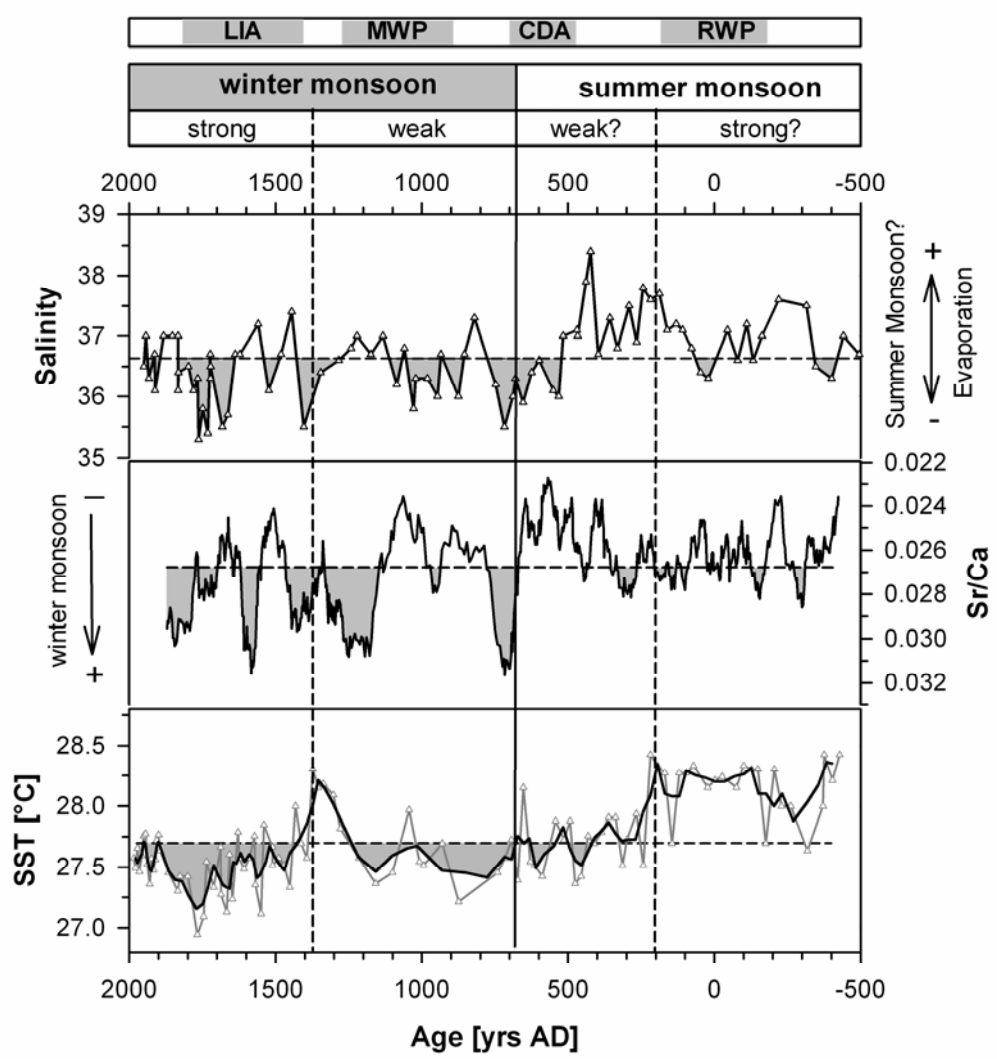
LIA
MWP
CDA
RWP
winter monsoon
summer monsoon
strong
weak
weak?
strong?
2000
1500
1000
500
0
-500
Salinity
39
38
37
36
35
Summer Monsoon?
+
-
Evaporation
winter monsoon
-
+
0.022
0.024
0.026
0.028
0.030
0.032
Sr/Ca
SST [°C]
28.5
28.0
27.5
27.0
Age [yrs AD]

Figure 5

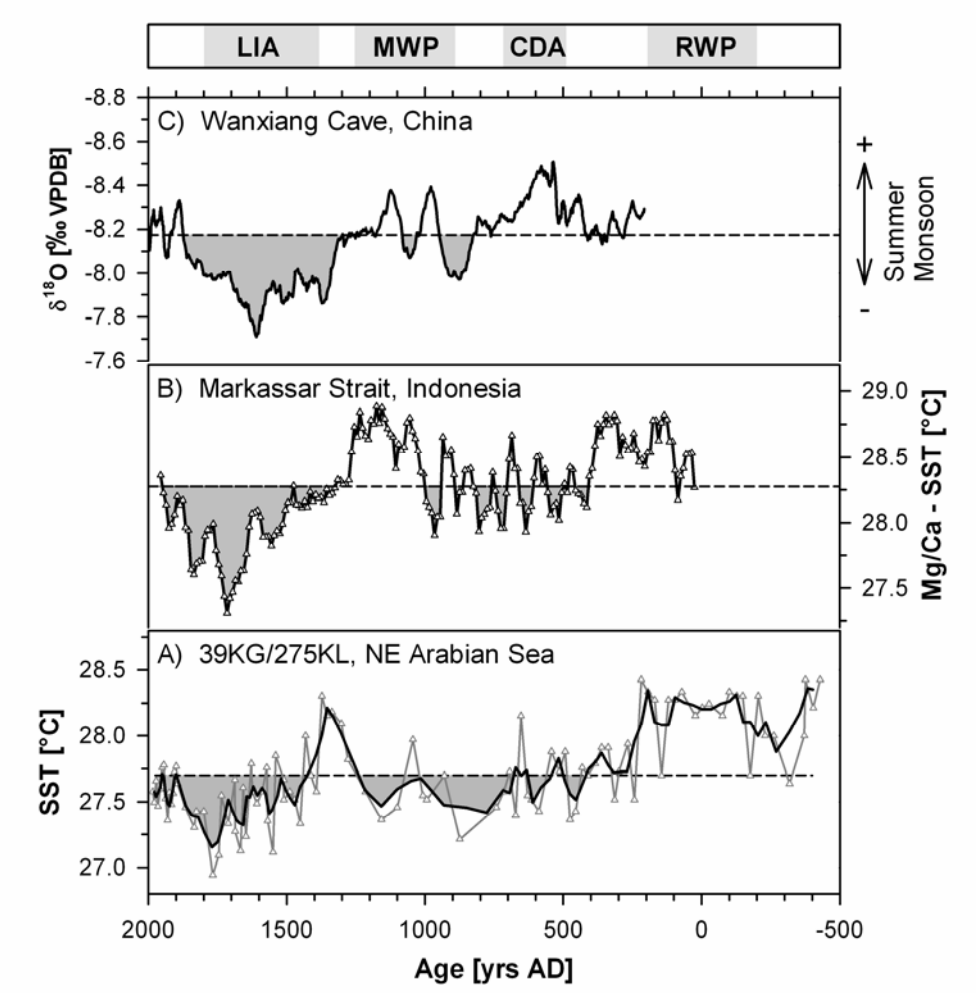
LIA
MWP
CDA
RWP
C) Wanxiang Cave, China
δ18O [‰ VPDB]
-8.8
-8.6
-8.4
-8.2
-8.0
-7.8
-7.6
+
Summer
Monsoon
-
B) Markassar Strait, Indonesia
29.0
28.5
28.0
27.5
Mg/Ca - SST [°C]
A) 39KG/275KL, NE Arabian Sea
SST [°C]
28.5
28.0
27.5
27.0
2000
1500
1000
500
0
-500
Age [yrs AD]

Figure 6